ARTICLE

BIOTECHNOLOGY and BIOENGINEERING

A Unique and Potent Protein Binding Nature of Liposome Containing Polyethylenimine and Polyethylene Glycol: A Nondisplaceable Property

Yen-Ku Liu,[1] Yu-Ling Lin,[1] Chia-Hung Chen,[1] Ching-Min Lin,[2] Kuan-Lun Ma,[1] Fu-Hsuan Chou,[2] Jin-Sheng Tsai,[3] Hsin-Yu Lin,[3] Fu-Rong Chen,[4] Tian-Lu Cheng,[5] Chia-Ching Chang,[2,6] Kuang-Wen Liao[1,2]

[1]Institute of Molecular Medicine and Bioengineering, National Chiao Tung University, Hsin-Chu, 30068, Taiwan, Republic of China; e-mail: liaonms@pchome.com.tw

[2]Department of Biological Science and Technology, National Chiao Tung University, Hsin-Chu, 30068, Taiwan, Republic of China; tel.: +886-3-5712121 (extn 56956); fax: +886-3-5729288,

[3]National Synchrotron Radiation Research Center, Hsin-Chu, 30068, Taiwan, Republic of China

[4]Department of Engineering and System Science, National Tsing Hua University, Hsin-Chu, 30068, Taiwan, Republic of China

[5]Department of Biomedical Science and Environmental Biology, Kaohsiung Medical University, Kaohsiung, 807, Taiwan, Republic of China

[6]Institute of Physics, Academia Sinica, Taipei, 11529, Taiwan, Republic of China

Received 23 September 2010; revision received 30 November 2010; accepted 20 December 2010

Published online 29 December 2010 in Wiley Online Library (wileyonlinelibrary.com). DOI 10.1002/bit.23048

ABSTRACT: Most of the currently available targeting vectors are produced via the linkage of targeting molecules. However, the coupling process is complicated, and the covalent linkage may attenuate the activity of certain targeting molecules. In this study, we have developed a cationic liposome complexed with polyethylenimine and polyethylene glycol polymers (LPPC) that can capture various proteins without covalent conjugation. Characterizations of prepared LPPC revealed that the maximal-binding capacity was about 170 μg of bovine serum albumin to 40 μg of sphere-shaped LPPC (180 nm). The proteins were essentially located at or near the surface when analyzed by atomic force or transmission electron microscopy. We demonstrate that polyethylenimine was an essential component to bind the proteins. Upon the saturation of captured proteins, a given protein could not be displaced by other additional proteins and still retained its biological activity. Using a variety of functional proteins, we show some typical examples of the utility of incorporated beta-glucuronidase and antibodies onto the LPPC. The beta-glucuronidase can be used for the study of antigen–antibody interactions, whereas in studies with the antibody complex, we used anti-CD3 as an agonist to stimulate the proliferation of peripheral blood mononuclear cells via a receptor-mediated mechanism and anti-VEGFR for cell staining. In conclusion, the prepared LPPC can provide a platform to capture biologically and biochemically functional proteins on its surface for various applications, such as cell signaling, cell profiling, noncovalent enzyme-linked immunoassays, and others not mentioned. Biotechnol. Bioeng.

Biotechnol. Bioeng. 2011;108: 1318–1327.

KEYWORDS: liposomes; lipid coating; polyethylenimine; protein capturing; cell staining

Introduction

Biocompatible and biodegradable liposomes are one of the established materials for delivering genes and drugs. Some cationic lipids are currently incorporated into the liposomes to enhance the efficiency of delivery (Kovacs et al., 2009; McNeil et al., 2010; Rao 2010; Semple et al., 2010). Several strategies, such as adding amino acid-based lipids (Obata et al., 2010) or cholesterol (Zidovska et al., 2009) into liposomes, have been developed to increase transfection efficiency. Other methods, including the modification of liposomes with arginine (Kim et al., 2010; Zhang et al., 2006) or polyethylenimine (PEI; Heyes et al., 2007; Pelisek et al.,

Yen-Ku Liu and Yu-Ling Lin contributed equally to this study

Correspondence to: Kuang-Wen Liao

Contract grant sponsor: National Science Council, Taiwan, ROC

Contract grant number: NSC 97-2313-B-009-002 and 98W962

2006; Schafer et al., 2010; Yamazaki et al., 2000), have also been reported. In addition, the specific delivery of liposomes to enhance the therapeutic efficacy of drugs is improved using covalent conjugation of the following peptides and proteins: arginine–glycine–aspartic acid peptides (bind to $\alpha_v\beta_3$ integrins; Temming et al., 2005; Zhao et al., 2009), GE11 peptides (bind to epidermal growth factor receptor; Song et al., 2008), mutant soluble B-cell activating factor from the TNF family (mBAFF) motif peptides (bind to the BAFF receptor, Zhang et al., 2008), and targeting antibodies, including anti-vascular cell adhesion molecule (Gosk et al., 2008) and anti-membrane type 1 metalloprotease antibodies (Hatakeyama et al., 2007).

Most of the currently available targetable liposomes are produced via the covalent linkage of targeting molecules onto liposomal components (Gosk et al., 2008; Hatakeyama et al., 2007; Song et al., 2008; Weng et al., 2008; Zhang et al., 2008; Zhao et al., 2009). This process may attenuate the activity of certain targeting molecules during the coupling reaction (Kocbek et al., 2007; Nobs et al., 2004; Zeng et al., 2007). One way to avoid this drawback involves the noncovalent adhesion of targeting molecules to a cationic liposome. However, the defluxion of targeting molecules from the liposomes, due to weak interactions between the targeting molecules and liposomes, poses another issue influencing the specific activity of the targeting liposome (Nobs et al., 2004; Sun et al., 2008).

In this study, we report a new polycationic liposome containing PEI and polyethylene glycol complex (LPPC) that can capture the targeting proteins via a noncovalent linkage without defluxion. We demonstrate that PEI polymers are located near the surface of prepared LPPC and offer remarkable electrostatic forces and hydrogen bonds to capture the proteins. When saturated with proteins, the complex provides a structural barrier for preventing incorporation of other protein molecules. Remarkably, the interaction between LPPCs and captured proteins could not be disrupted, even after competition with a 10-fold excess of bovine serum albumin (BSA). To our knowledge, this is the first report showing that bound proteins cannot be displaced by unbound proteins. Furthermore, we illustrate some potential utilities of this technology using functional immunoglobulin for cell activation and staining and specific antibodies and enzymes, such as beta-glucuronidase, for enzyme-linked immunosorbent assay (ELISA).

Materials and Methods

Reagents

1,2-Dioleoyl-*sn*-glycero-3-phosphocholine (DOPC) and 1,2-dilauroyl-*sn*-glycero-3-phosphocholine (DLPC) were purchased from Avanti Polar Lipids (Alabaster, AL). Polyethylene glycol (PEG, MW 1,500 and 8,000), polyethylenimine (PEI branched, MW 25,000), para-nitrophenyl-β-D-glucuronide (PNPG), and 3,3'-dioctadecyloxacarbocyanine (DiO) were from Sigma–Aldrich (St. Louis, MO). BSA was purchased from Invitrogen (Gaithersburg, MD). HRP-conjugated rabbit IgA was purchased from Acris Antibody GmbH (Herford, Germany). Rabbit polyclonal antibody to the DDR1 peptide was purchased from Abnova (Taipei, Taiwan). Anti-CD28 antibody was purchased from Biolegend (San Diego, CA). Anti-VEGF receptor 1 antibody (Flt-1/EWC) was purchased from Abcam (Cambridge, UK).

Cell Lines and Tissue Culture

Peripheral blood mononuclear cells (PBMC) were collected using a Ficoll-Paque™ Plus (Amersham Biosciences, Uppsala, Sweden). The B16F10 and Balb/3T3 cell lines were obtained from the Food Industry Research and Development Institute (Hsin-Chu, Taiwan) and cultured in a humidified atmosphere of 5% CO_2 at 37°C according to a standard procedure previously described (Liao et al., 2003). Cell culture growth media, Dulbecco's Modified Eagle's Medium (DMEM; Invitrogen) and Roswell Park Memorial Institute (RPMI; Invitrogen) 1640 culture medium were supplemented with 10% heat inactivated fetal bovine serum (FBS; Invitrogen) and 1% penicillin/streptomycin/amphotericin (PSA; Biological Industries, Beithaemek, Israel).

The Preparation of Liposomes Containing Polyethylenimine (PEI) and Polyethylene Glycol (LPPC)

LPPC was prepared by coating an equal weight of DOPC and DLPC (total 50 mg) in 1 mL chloroform onto a round bottom flask using a rotary evaporator (EYELA; N-1000S, Tokyo, Japan) to yield a thin lipid film (Schafer et al., 2010; Tabatt et al., 2004). The film was hydrated with 5 mL of deionized water while dissolving an additional 675 mg PEI and 220 mg PEG-8000. At this stage, the molar ratio of phospholipids:PEI:PEG was about 13:5:5. Notably, any concentration of PEI greater than that mentioned above appears to be insoluble in water. The hydrated film was vigorously resuspended for 10 min, and the mixture was extruded 9 times through a LiposoFast extruder (Avestin Inc., Ottawa, ON, Canada) via a 200 nm membrane. The suspension was diluted 50-fold in deionized water and centrifuged at 5,900*g* for 5 min to remove any unincorporated materials. Finally, the pellets were resuspended with 5 mL deionized water and stored at 4°C. The amount of LPPC defined in the present study was solely based on the phospholipid content of the complex, unless otherwise mentioned.

Electron Microscopic Analyses and Characterizations of LPPC

Ten microliters of LPPC (200 μg/mL) was dropped and dried onto a formvar/carbon membrane without staining,

and morphologic features of LPPC particles were observed by transmission electron microscopy (TEM, JEOL1010F; JEOL Ltd., Tokyo, Japan) at 100 kV. For scanning electron microscopy (SEM), LPPC was dropped onto a silica wafer coated with platinum and scanned with an S-4700 SEM (Hitachi S-4700, Tokyo, Japan).

BSA-conjugated gold particles were prepared according to the reported procedure (Chuang et al., 2010). A solution of gold nanoparticles (AuNPs, 4.75 mL) was mixed with the BSA solution (0.1%, 0.25 mL) and incubated at 37°C for 2 h. The mixture was then centrifuged at 14,000*g* for 6 min to remove the excess BSA. Then 200 μg of LPPC or liposomes without polymers was incubated with 50 μg BSA-AuNPs and 750 μg BSA at 37°C for 20–30 min. Finally, 10 μL of each complex was dropped and dried onto a formvar/carbon membrane without staining, and the morphologic features of LPPC particles were observed by transmission electron microscopy (TEM, JEOL1010F; JEOL Ltd.) at 100 kV.

Atomic force microscopy (AFM; JPK Instruments, Berlin, Germany) was conducted using 10 μL of LPPC (200 μg/mL) or the LPPC–BSA complex (200 μg/mL LPPC and 750 μg/mL BSA). The LPPC or LPPC–BSA was dropped onto a freshly prepared mica sheet for 10 min at room temperature. An Al-coated Si cantilever (PPP-SEIHR-50; Nanosensors, Neuchâtel, Switzerland) with a spring constant of 5–37 N/m and a resonance frequency of 96–175 kHz was used for the measurement.

The particle size was determined using a BI-200SM dynamic laser light scattering goniometer (Brookhaven Inc., Holtsville, NY). The measurements of 2 mg of the various liposomes were taken in 200 μL deionized water before and after the centrifugations.

Determination of the Timing and Content of BSA Binding to LPPC

Forty micrograms of LPPC was incubated with 200 μg BSA for different times at 37°C and centrifuged at 5,900*g* for 5 min. The pellets were resuspended, and the quantity of BSA bound to LPPC was determined using a Coomassie Plus Bradford™ Assay Kit according to the standard procedures provided by the manufacturer.

Following the binding of BSA to LPPC in 1 mL deionized water, the complex was centrifuged at 5,900*g* for 5 min to remove unbound BSA, and the pellets were washed with 1 mL deionized water. The amount of bound BSA was measured as described above.

Isothermal titration calorimetry (ITC, Model 2277 TAM; TA Instruments, New Castle, DE) was used to monitor the heat released during the binding of BSA to LPPC at 25°C according to a standard procedure (de Rivera et al., 2009). BSA (10 mg/mL) was titrated into 200 μg LPPC in 2.8 mL deionized water at an injection speed of 1 μL/s and proceeded with additions of 10 μL per step.

Displacement Test

FITC-BSA (42 μg) and BSA (150 μg) were incubated with LPPC (40 μg) for 20–30 min at 37°C and then centrifuged at 5,900*g* for 5 min to remove any unincorporated FITC-BSA and washed. After resuspension, the LPPC–FITC–BSA complex was incubated with increasing amounts of unlabeled BSA (200–500 μg) for 20 min at 37°C. Following washes and resuspension, FITC-BSA on LPPC was monitored using a spectrophotometer (Ultrospec 3100; Amersham Biosciences) at 488 nm (excitation) and 515 nm (emission). A similar protocol was used to monitor whether beta-glucuronidase (βG; kindly provided by Dr. T L Cheng of Kaoshung Medical School, Taiwan) or HRP-labeled antibody incorporated into LPPC could be displaced in the presence of excess BSA. The activity of βG was measured by incubating the complexes with 200 μL of 0.3 mM PNPG for 20 min and measuring the absorbance at 450 nm (Chuang et al., 2006). The activity of HRP was measured by incubating the mixture with 100 μL of SureBlue™ TMB substrate (KPL, Gaithersburg, PA) for 20 min, stopping the reaction with 100 μL/well 1 N HCl, and reading the absorbance at 450 nm.

Forty micrograms of LPPC was incubated with 6 μg anti-CD3 antibody (2C11, kindly provided from Dr. Steve R. Roffler) and 100 μg BSA coupled to magnetic beads in 1 mL DMEM containing 10% FBS and 1% PSA at 37°C. After incubating for 3 days, the LPPC–antibody complex (pellet) and released antibody (supernatant) were separated by magnetic field. Each of the samples was treated with the Balb/c splenocytes, and the proliferation of the splenocytes was determined with the MTT assay. In addition, varying amounts of antibody were added to the splenocytes to generate a standard curve to calculate the percentage of antibodies released.

Protein-Binding Ability of LPPC Devoid of PEI or PEG

LPPC devoid of PEI or PEG was prepared from the lipid film as described above. After diluting the suspensions 50-fold, unincorporated materials were removed by a centrifugation at 5,900*g* for 5 min followed by the addition of 5 mL deionized water to resuspend the pellets. Forty micrograms of each liposome was incubated with 10 μg HRP-conjugated antibody and unlabeled antibody or excess BSA (over 100 μg) to occupy the unreacted sites of the liposomes for 20 min at 37°C. After removal of any unbound antibody or BSA by centrifugation, the pellet was washed with 1 mL deionized water. HRP activity was measured as described above.

LPPC was incubated at 4, 25, and 37°C for up to 5 days. At each time point, the protein-binding capacity of LPPC (40 μg) was measured by incubating the LPPC with 200 μg of BSA for 20–30 min at 37°C. Following washes and resuspension, the amount of bound BSA was measured as described above.

Cell Proliferation of LPPC Complexed With Anti-CD3 and Anti-CD28 Combined With Anti-CD3

PBMC were seeded in a 96-well plate at 1×10^5 per well in 100 μL RPMI medium containing 10% FBS and 1% PSA. LPPC (40 μg) was initially incubated with 2.4 μg of anti-CD3 monoclonal antibody (OKT3, kindly provided from Dr. Steve R. Roffler) or 2.4 μg of anti-CD3 combined with 2.4 μg of anti-CD28 in a final volume of 100 μL. The mixture was then treated with BSA in excess (over 100 μg) for 20 min at 37°C to block the unreacted sites of LPPC and washed by centrifugation at 5,900*g* for 5 min. To stimulate the proliferation of PBMC, 2.5 μL LPPC (1 μg) complexed with antibody were added into each PBMC-seeded well and incubated for 3 days. The MTT test was performed to measure the proliferation rate of PBMC. The concentrations of INF-γ and IL-2 secreted by stimulated PBMC were determined by commercial kits (DuoSet ELISA, R&D System, Minneapolis, MN). LPPC alone or free monoclonal antibodies (mAb) of equal amounts were added to separate wells as negative controls.

Noncovalent ELISA

Each well in a 96-well plate was coated with 1 μg (or the amount mentioned in the figure) of heat shock protein 60 (Hsp60) overnight and blocked with 2% skim milk. LPPC (40 μg) was complexed with 2 μl βG (2.2 mg/mL) and 2 μL anti-Hsp60 antibody (4 mg/mL, provided by our lab) in a final volume of 10 μL for 30 min at 37°C and then blocked with 20 μL PEG-1500 (100 mg/mL) for another 30 min to reduce nonspecific binding (Lin et al., 2010). The mixture was then centrifuged at 5,900*g* for 5 min, and washed. The pellets of the LPPC complexes were resuspended in 20 μL deionized water, mixed with 100 μL PBS, and added to each well. After incubation for 30 min, the 96-well plate was washed with PBST (0.05% Tween-20) twice and developed by the addition of 200 μL of 0.3 mM PNPG for 20 min as mentioned above. For detection of various amounts of coating proteins, 20 μg of LPPC complexed with 2 μL βG (2.2 mg/mL) and 0.3 μL antibody (4 mg/mL) was utilized in each well following the procedure mentioned above.

Utility of Immunostaining for Flow Cytometry

To study the binding ability of LPPC to the surface of a given cell, LPPC was first incorporated by 3 mM fluorescent lipophilic dye DiO (10 μL in 1 mg LPPC with a final volume of 110 μL) for 30 min followed by washes and resuspension as described above. Next, 2 μL of DiO-incorporated LPPC (20 μg) was complexed with 2 μg of an anti-VEGF receptor 1 antibody (Flt-1/EWC) or 2 μg of an unrelated antibody (anti-DDR1 antibody) as a negative control using procedures similar to those mentioned above and then blocked with 20 μL PEG-1500 (100 mg/mL) for another 30 min. Mouse B16 melanoma cells containing the VEGF receptor-1 (5×10^5 per tube; Gille et al., 2007) or Balb/3T3 cells without VEGF receptor-1 (5×10^5 per tube) were treated with the LPPC complex at 4°C for 30 min in the dark. Following washes and resuspension in 1 mL DMEM, the cells were analyzed using a FASCcan flow cytometer (Becton Dickinson, San Jose, CA).

Statistical Analysis

Data were analyzed using an SAS statistical software package (SAS Institute, Inc., Cary, NC). A *t*-test was used when comparing two independent trials, while an ANOVA test was used for comparing multiple variables. Differences of $P < 0.05$ were considered statistically significant. All of the results were expressed as the mean ± SD.

Results and Discussions

Formation and Characterization of LPPC

DLPC and DOPC have been recently used for liposome preparation (Bennun et al., 2008; Lin et al., 2006; Mangala et al., 2009; Merritt et al., 2008). One of the requirements of the liposomes used in this study is that the excess unconjugated proteins need to be removed following the incorporation. Figure 1A shows that liposomes composed of DOPC or DLPC plus DOPC, but not DLPC alone, could be pelleted by centrifugation. Therefore, we mixed equal weights of DLPC with DOPC for the preparation of our liposomes. Under this condition, the excess proteins can be "washed away" by centrifugation. According to our results, PEI can combine with PEG, and we propose that such polymers may surround the liposome to form a cationic lipoplex. To generate cationic liposomes, the lipid mixture was then complexed with PEI and PEG polymers according to the procedures mentioned above. The optimized molar ratio of phospholipids to PEI and PEG polymers was 13:5:5 to efficiently capture the proteins (data not shown). As expected, liposomes complexed with PEI and PEG (LPPC) can also be pelleted (Fig. 1A), but PEI or PEG alone could not. The amounts of PEI and PEG incorporated into the LPPC were determined, and the final molar ratio of phospholipids to PEI and PEG polymers was found to be 13:0.05:0.5 (or 6.75 mg PEI and 22 mg PEG per 50 mg phospholipids). In addition, when examined under TEM, the surface of the LPPC particles was sphere-shaped and surrounded by electron-dense materials (Fig. 1B), but liposomes without polymers were not (Fig. 1C). The average size of prepared LPPC was about 180 nm in diameter, as displayed by SEM (Fig. 1D) and consistent with that measured by dynamic laser scattering (179.5 ± 13.7 nm, a major peak of Fig. 1E), but few were over 500 nm.

Next, we measured the surface voltage potential of our cationic LPPC with a Zetasizer. A value of 40.1 ± 9.5 mV was observed, suggesting that the surface of LPPC is highly

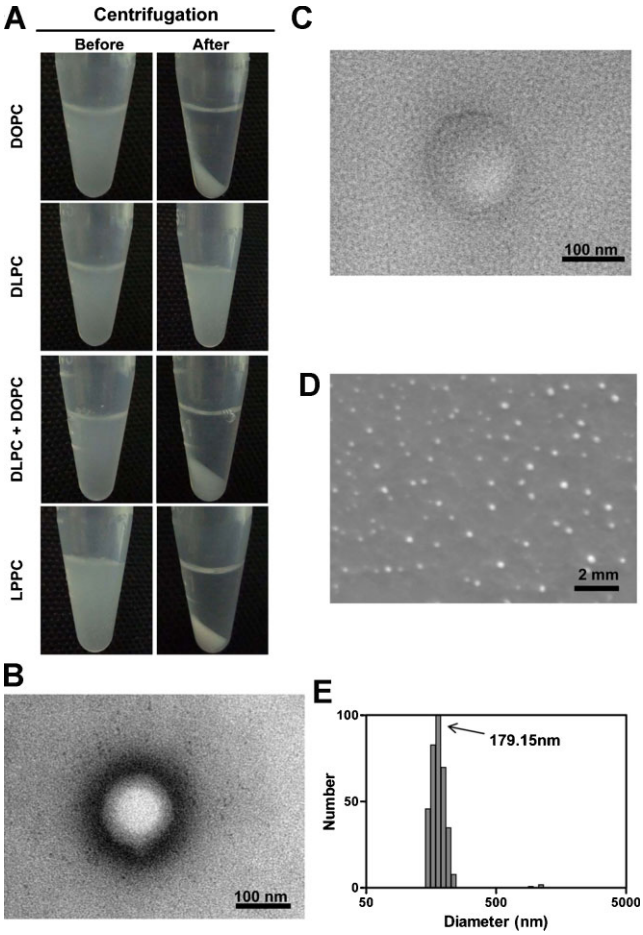

Figure 1. Characterization of LPPC. **A**: The photographs of various liposomes are displayed before and after centrifugation at 5,900*g* for 5 min. The transmission electron micrographs were taken from samples of (**B**) liposomes complexed with PEI and PEG (LPPC), and (**C**) liposomes without polymers. The surface of an LPPC particle was surrounded by electron-dense materials but that of a liposome alone was not. Plots of the size distributions of LPPCs are displayed from (**D**) scanning electron microscopy and (**E**) dynamic laser light scattering. [Color figure can be seen in the online version of this article, available at http://wileyonlinelibrary.com/bit]

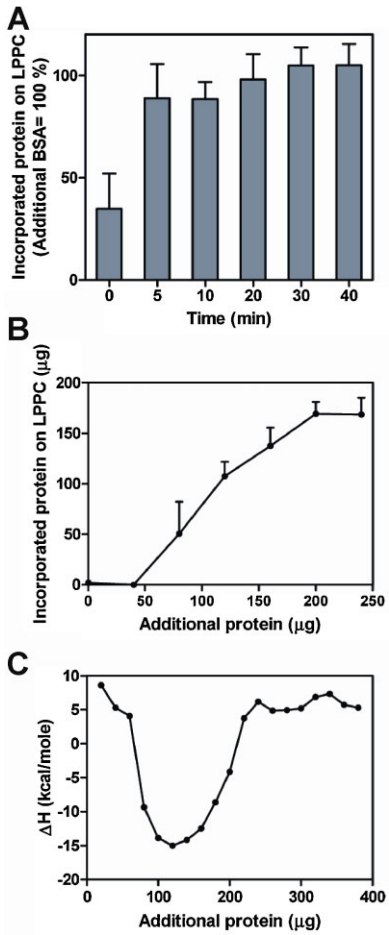

Figure 2. BSA-binding ability of LPPC. **A**: LPPC (40 μg) was incubated with 200 μg BSA for different times, and the amount of bound protein was analyzed with the Bradford Assay. **B**: LPPC (40 μg) was incubated with different amounts of BSA for 30 min, and the amount of bound protein was analyzed with the Bradford Assay. **C**: LPPC (40 μg) was incubated with 20 μg BSA every 20 min, and the energy variation was detected by isothermal titration calorimetry. Shown is the mean ± SD of three independent experiments performed in duplicate.

positively charged, similarly to other cationic liposomes (Schafer et al., 2010; Wang et al., 2010).

Binding of BSA to LPPC

Sequentially, we examined whether LPPC was able to capture proteins using BSA as a reference. First, we found that after adding BSA to LPPC and incubating over time at 37°C, the maximal binding was achieved within 30 min (Fig. 2A). The capacity of LPPC (40 μg in 1 mL) for BSA incorporation following a 20 min incubation was then determined. Figure 2B shows that the amount of BSA incorporation could be saturated in a concentration-dependent manner. The maximal binding capacity was 168.6 ± 16.4 μg of BSA to 40 μg of LPPC or a binding ratio about 4:1 (w/w). Second, we investigated the energy released using an ITC measurement while mixing LPPC with BSA. Figure 2C reveals that heat was released starting at a critical concentration of BSA (40 μg), indicating that BSA binding to LPPC began at this point and terminated after 200 μg BSA was added. Interestingly, this coincides with the results from Figure 2B. Finally, we investigated the surface of LPPC with and without the incorporation of BSA using AFM analysis. Figure 3A and B depicts that the BSA–LPPC complex possessed a rough and raised surface relative to the smooth surface of LPPC alone. We suggest that the captured BSA is located at or near the surface of LPPC. To further visualize the incorporated BSA, BSA-conjugated gold particles were utilized as markers. We show that BSA-gold particles were located on surface of LPPC using TEM without negative staining (Fig. 3C and D) but not on liposomes without polymers. This indicates that the proteins might be bound through polymers and that the binding occurs on the surface of the LPPC particle.

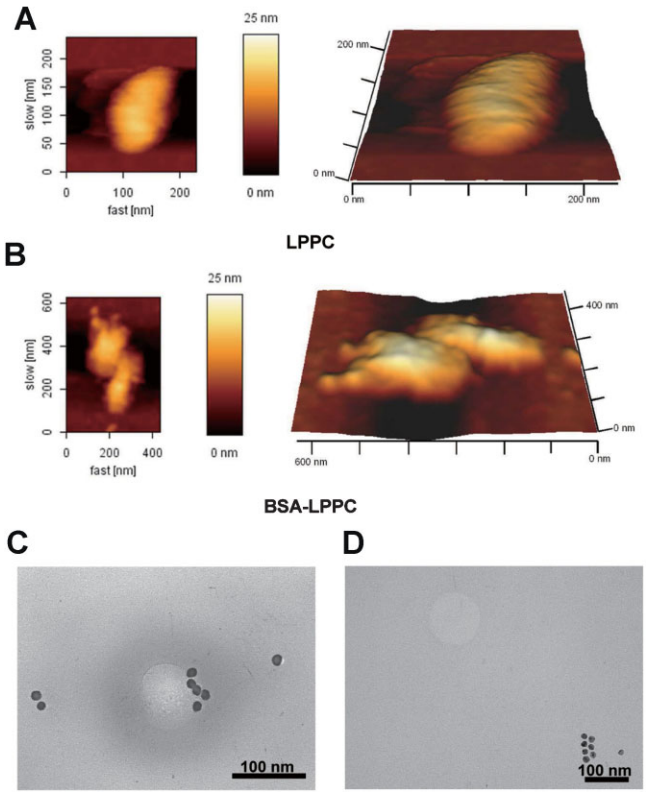

Figure 3. Images of protein–LPPC complexes by atomic force microscopy (AFM) or transmission electron microscopy (TEM). The AFM images were taken from samples of (**A**) LPPC alone and (**B**) BSA–LPPC complexes. The results show that the surface of the BSA–LPPC complex is less regularly shaped. The scale for particle height is represented in color. The TEM images were taken after incubating the BSA-modified gold particles with (**C**) LPPC or (**D**) liposomes without polymers. [Color figure can be seen in the online version of this article, available at http://wileyonlinelibrary.com/bit]

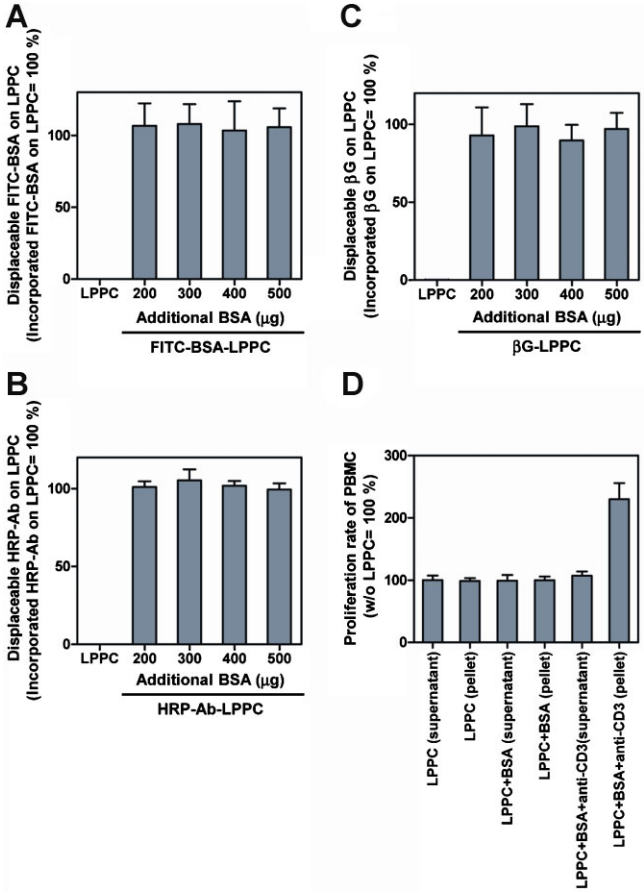

Figure 4. Nondisplaceable binding of proteins to LPPC. **A**: FITC-conjugated albumin (FITC-BSA), (**B**) an HRP-conjugated antibody (HRP-Ab), or (**C**) beta-glucuronidase (βG) was previously incorporated on LPPC, and the protein–LPPC complexes were treated with different amounts of BSA in 1 mL final volume. Following centrifugation, the percentage of nondisplaceable protein on LPPC was measured. LPPC is the background of LPPC alone. **D**: Antibody–LPPC complexes were incubated in serum containing media for 3 days, and the nondisplaceable antibody on LPPC (pellet) was able to stimulate the proliferation of PBMC. Shown is the mean ± SD of three independent experiments performed in duplicate.

Nondisplaceable Binding of BSA to LPPC

We tested whether the BSA bound to LPPC could be displaced or exchanged by exogenously added BSA. FITC-conjugated BSA (used as a probe to monitor the binding) was initially complexed with LPPC at a saturating concentration (200 μg/mL) similar to that described in Fig. 2B. The results show that once FITC-BSA was incorporated into the LPPC, it was not displaced by the unconjugated BSA, even in the presence of excess amounts of protein (Fig. 4A).

Nondisplaceable Binding of Antibody or Enzyme to LPPC

Using the same strategy mentioned above, we tested whether LPPC complexed with an antibody (HRP-labeled antibody) or an enzyme (βG) was also nondisplaceable in the presence of excess BSA. An antibody labeled with HRP was used because its activity could be detected with a chromogenic substrate. Again, BSA was not able to displace or compete with the antibody or enzyme that had already associated with LPPC (Fig. 4B and C). In addition, we show that the incorporated antibody retained its activity while associated with the LPPC in serum-containing media for 3 days. Only 0.6% of this antibody was released into serum after the 3-day incubation (Fig. 4D). A bound antibody (HRP-labeled antibody), FITC-conjugated BSA, or enzyme (βG) could not be displaced by excess BSA or any of the many proteins found in serum (Fig. 4A–D). Taken together, we have established a cationic liposome with the ability to bind proteins that cannot be displaced by other additional proteins.

Role of PEI in the Formation of LPPC Protein Complex

To identify which component of LPPC was responsible for the binding of a given protein to LPPC, we prepared a

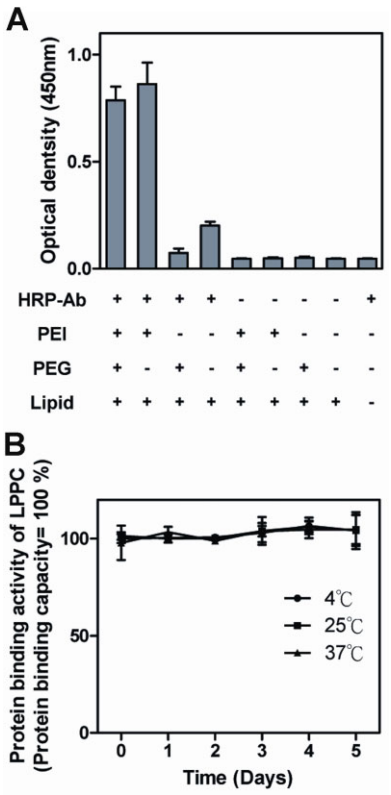

Figure 5. Role of polyethylenimine (PEI) in protein-binding ability. **A**: Phospholipid liposomes devoid of either PEI or PEG were tested for their ability to bind HRP-conjugated antibodies (HRP-Ab), and the results show that PEI is the key component contributing to the binding ability. **B**: The LPPC was incubated with 200 μg BSA for various times, and the amount of bound protein was analyzed with the Bradford Assay. The binding activity of LPPC is not significantly different. Shown is the mean ± SD of three independent experiments performed in duplicate.

phospholipid liposome devoid of either PEI or PEG and tested its ability to bind to the HRP-labeled antibody. Figure 5A clearly demonstrates that PEI is an extremely essential component mediating binding to the antibody and playing a key role in the uptake of protein in our prepared LPPC. For this reason, we monitored the stability of PEI in LPPC when LPPC was stored at 4 and 37°C over a period of up to 30 days by centrifuging LPPC to separate possible unassociated PEI. In this experiment, the content of PEI was determined using a ninhydrin test. We found that there were no significant changes in PEI content relative to freshly prepared LPPC. In addition, we tested BSA binding to LPPC at 4, 25, and 37°C for 5 days. Figure 5B shows that there were no significant changes in BSA-binding ability, indicating that the PEI incorporated on LPPC was stable. We also stored LPPC at 4°C for 30 days and further examined its protein-binding ability, and we found that there were no significant differences in protein-binding relative to freshly prepared LPPC (data not shown).

With respect to the orientation of PEI over the LPPC, we found several lines of evidence indicating that the LPPC particle surface was at least in part surrounded by PEI. First, the ninhydrin test indicated that primary amines, which only exist in PEI, were detected in LPPC. This could only be explained if PEI existed in LPPC. Second, PEI is a key component in the adsorptive ability of LPPC (Fig. 5A). Third, the results from AFM and TEM suggest that the proteins were bound onto or near the surface of LPPC (Fig. 3A–D). Moreover, TEM showed that the surface of LPPC was surrounded with electron-dense material, indicating that the polymer may be present (Figs. 1B and 3C). Taken together, these results indicate that PEI polymers of LPPC should exist on the surface of LPPC and play a pivotal role in protein binding.

How PEI prevents protein displacement by other proteins (at the saturation point) remains elusive. Nonetheless, several possibilities may explain the mechanism governing this observation. First, the bound protein may be captured by numerous electrostatic forces and hydrogen bonds provided by PEI (Khoo et al., 2009; Ong et al., 2009), and it may be difficult to simultaneously overcome all of these forces to dissociate the pre-captured proteins from the liposome. Second, the binding of a given protein on LPPC after the saturation point could result in a steric barrier to the subsequent additional proteins. Third, a large number of tiny branches of PEI on prepared liposomes (Fig. 1B) might firmly interact with the microstructure of an individual protein like a "Velcro-like" fastener (Creze et al., 2008; Durrieu et al., 2008).

Utility of Biologically Active Protein Complexed With LPPC

Next, we tested whether biologically functional proteins could bind LPPC and still maintain their functions. First, we chose the anti-CD3 and anti-CD28 antibodies as two representative examples. Either anti-CD3 or anti-CD3 combined with anti-CD28 is known to be a mitogen stimulating the proliferation of PMBCs via the receptor-mediated mechanism, in which the proliferative potency of anti-CD3 can be intensified in the presence of anti-CD28 (Yamada-Ohnishi et al., 2004). Figure 6A shows that LPPC complexed with these agonists not only retained its ability to stimulate the proliferation of PBMC in serum-containing media, but also exhibited biological activity similar to that of unbound anti-CD3 or anti-CD3 combined with anti-CD28. In addition, the complex was also capable of triggering cytokine release from PBMCs as expected, and amounts of released INF-γ or IL-2 were comparable to those released after treatment with unbound antibodies (Fig. 6B and C). These results indicate that LPPC did not impair the activities of bound antibodies and imply that such immuno-LPPC complexes may have the potential to be applied in immunotherapy to regulate immunity.

Utility of a Noncovalently Linked Enzyme Immunoassay

The ELISA has been a common method for monitoring the antigen–antibody interaction. However, the procedures

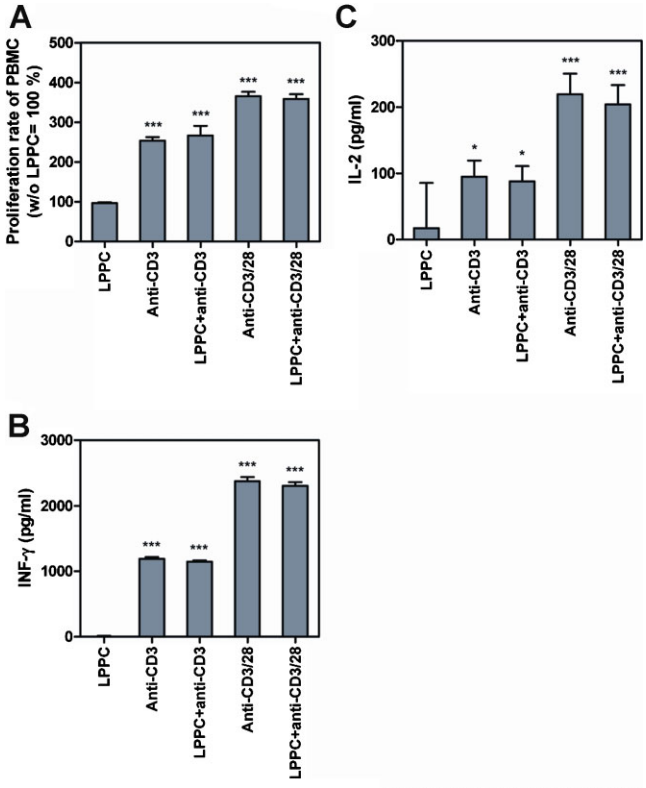

Figure 6. Stimulation of peripheral blood mononuclear cells (PMBC) with antibody–LPPC complexes. Human PBMCs were treated with unbound antibodies or LPPC-bound antibodies, and (**A**) the proliferation rates of treated cells were measured by an MTT assay. In addition, release of (**B**) INF-γ and (**C**) IL-2 from treated cells was determined by ELISA. Shown is the mean ± SD of three independent experiments performed in duplicate ($^{*}P < 0.05$; $^{***}P < 0.001$).

involved in the addition of a primary antibody and a covalent enzyme-linked secondary antibody are relatively time consuming. We herein co-incorporated an enzyme (βG) and an antibody into our LPPC without a covalent linkage to mimic the nature of an "enzyme-linked antibody". Figure 7A provides an example that LPPC complexed with both βG and an antibody can monitor the antigen–antibody binding on an ELISA plate and that the assay can be completed within a short period of time without using a conventionally prepared enzyme-labeled secondary antibody. Moreover, Figure 7B shows that the chromogenic density occurred in a concentration-dependent manner and that this potent strategy exhibited high sensitivity, detecting even 1 pg antigen.

Utility of Immunostaining for Flow Cytometry

We provide another example of the use of LPPC for cell staining. In this experiment, we first incorporated a lipophilic fluorescent dye (presumably into liposomal core), DiO, to generate a "fluorescently-tagged" LPPC. A monoclonal antibody against VEGF receptor-1 [Flt-1/EWC]

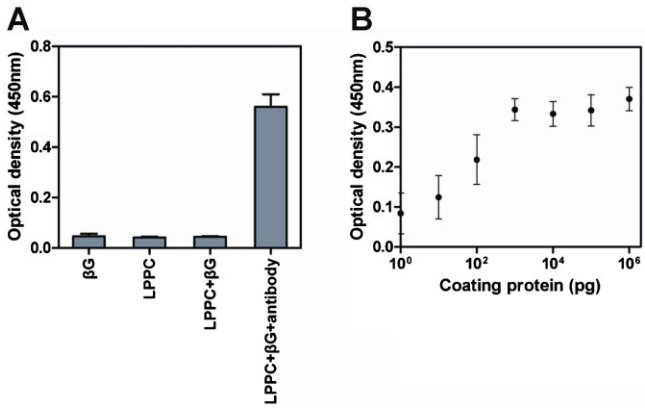

Figure 7. Noncovalently linked enzyme immunoassay of antibody-LPPC complexes. **A**: LPPC bound with anti-heat shock protein 60 (Hsp60) antibody and βG, or with either one individually, was incubated with 1 μg Hsp60 coated on the wells of a 96-well microtiter plate. After adding the substrates, βG activities were measured to determine the targeting abilities. βG is the background of the assay system. **B**: LPPC incubated with different amounts of Hsp60 was also analyzed. The data shown here have been obtained by subtracting the background from the original value. Shown is the mean ± SD of three independent experiments performed in duplicate.

was then captured onto the LPPC. The antibody–DiO–LPPC complex was then incubated with mouse B16 melanoma cells containing the VEGF receptor-1 (Gille et al., 2007) and mouse embryonic fibroblasts (Balb/3T3) as a negative control, respectively. Figure 8A shows that by flow cytometric analysis, cells were labeled by this LPPC complex, but not by the LPPC complexed with DiO alone or complexed with DiO and a nonrelated antibody, which was used as a negative control. As expected, mouse Balb/3T3 embryonic fibroblasts were not targeted by the LPPC complex either. These results reveal that antibody–LPPC complexes not only possess the potential to bind a specific

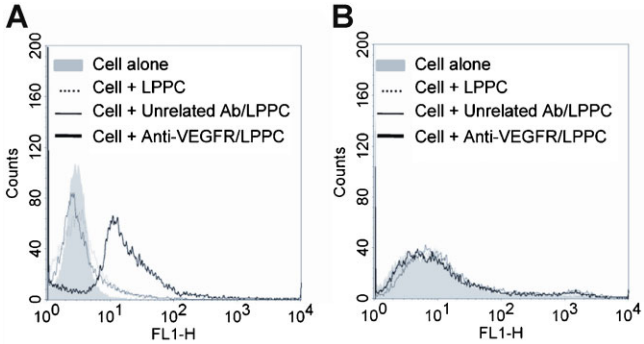

Figure 8. Cell targeting of antibody–DiO–LPPC complexes. **A**: B16 melanoma cells or (**B**) embryonic fibroblasts were stained with the DiO-labeled LPPC complex with or without antibodies. The anti-VEGFR1 antibody–DiO–LPPC complex targeted the B16 melanoma cells, but other complexes did not. Grey shadow: the cell alone. Black dotted line: the LPPC alone. Black thin line: the LPPC complexed to an unrelated antibody. Black thick line: LPPC complexed to an anti-VEGFR1 antibody. A representative example of three independent experiments performed in duplicate is shown.

surface antigen of a given cell but also provide an opportunity for the use of flow cytometric analyses. The latter technique is usually involved in the preparation of fluorescently labeled secondary antibodies.

The combination of targeting molecules, such as targeting peptides or antibodies, with liposomes has been utilized to enhance the efficiency of drug or DNA delivery (Gosk et al., 2008; Hatakeyama et al., 2007; Temming et al., 2005; Zhao et al., 2009). Covalently linking the target molecules to liposomes is a prevalent method of conjugation, but this process may attenuate the activity of certain targeting molecules (Kocbek et al., 2007; Nobs et al., 2004; Zeng et al., 2007). Noncovalent combination is another convenient method, but this interaction is too weak to stabilize the molecules on the particles (Nobs et al., 2004; Sun et al., 2008). In our study, LPPC possesses the ability to stably bind proteins through noncovalent interactions, which provides several advantages. First, LPPC not only stably binds proteins but also retains their activities (Fig. 4A–D). With these unique properties, LPPC complexed with antibodies could be utilized as an immuno-liposome in a noncovalently linked enzyme immunoassay (Figs. 6 and 7). Second, LPPC could be used in small-volume applications to complex lipophilic fluorescent dyes. Thus, it is convenient to use these complexes as probes for cell staining (Fig. 8). Finally, LPPC can be centrifuged to form a pellet, allowing LPPC to be easily separated from the unincorporated molecules to avoid the interference of free proteins (Sun et al., 2008).

Conclusions

We have developed a novel cationic and spherical LPPC that can tightly capture proteins on or near its surface as evidenced by AFM and TEM analyses. PEI polymers play a key role for the protein binding to LPPC. Of remarkable interest, the proteins associated onto protein–LPPC complexes could not be displaced. Although the exact mechanisms for this nondisplaceable nature from the LPPC are not yet clear, the prepared LPPC could provide a platform to capture biologically and biochemically functional proteins on its surface for various applications, such as cell signaling, cell profiling and noncovalent enzyme-linked immunoassays.

This work was supported by the National Science Council, Taiwan, R.O.C. (NSC 97-2313-B-009-002 and 98W962). We would like to thank Drs. Steve R. Roffler and Tian-Lu Cheng for kindly providing beta-glucuronidase, 2C11, and OKT3 antibodies.

References

Bennun SV, Faller R, Longo ML. 2008. Drying and rehydration of DLPC/DSPC symmetric and asymmetric supported lipid bilayers: A combined AFM and fluorescence microscopy study. Langmuir 24:10371–10381.

Chuang KH, Cheng CM, Roffler SR, Lu YL, Lin SR, Wang JY, Tzou WS, Su YC, Chen BM, Cheng TL. 2006. Combination cancer therapy by hapten-targeted prodrug-activating enzymes and cytokines. Bioconjug Chem 17:707–714.

Chuang YC, Li JC, Chen SH, Liu TY, Kuo CH, Huang WT, Lin CS. 2010. An optical biosensing platform for proteinase activity using gold nanoparticles. Biomaterials 31:6087–6095.

Creze C, Castang S, Derivery E, Haser R, Hugouvieux-Cotte-Pattat N, Shevchik VE, Gouet P. 2008. The crystal structure of pectate lyase PelI from soft rot pathogen *Erwinia chrysanthemi* in complex with its substrate. J Biol Chem 283:18260–18268.

de Rivera MR, Socorro F, Matos JS. 2009. Heats of mixing using an isothermal titration calorimeter: Associated thermal effects. Int J Mol Sci 10:2911–2920.

Durrieu MP, Lavery R, Baaden M. 2008. Interactions between neuronal fusion proteins explored by molecular dynamics. Biophys J 94:3436–3446.

Gille J, Heidenreich R, Pinter A, Schmitz J, Boehme B, Hicklin DJ, Henschler R, Breier G. 2007. Simultaneous blockade of VEGFR-1 and VEGFR-2 activation is necessary to efficiently inhibit experimental melanoma growth and metastasis formation. Int J Cancer 120:1899–1908.

Gosk S, Moos T, Gottstein C, Bendas G. 2008. VCAM-1 directed immunoliposomes selectively target tumor vasculature in vivo. Biochim Biophy Acta Biomembr 1778:854–863.

Hatakeyama H, Akita H, Ishida E, Hashimoto K, Kobayashi H, Aoki T, Yasuda J, Obata K, Kikuchi H, Ishida T, Kiwada H, Harashima H. 2007. Tumor targeting of doxorubicin by anti-MT1-MMP antibody-modified PEG liposomes. Int J Pharm 342:194–200.

Heyes J, Palmer L, Chan K, Giesbrecht C, Jeffs L, MacLachlan I. 2007. Lipid encapsulation enables the effective systemic delivery of polyplex plasmid DNA. Mol Ther 15:713–720.

Khoo KS, Teh EJ, Leong YK, Ong BC. 2009. Hydrogen bonding and interparticle forces in platelet alpha-Al2O3 dispersions: Yield stress and zeta potential. Langmuir 25:3418–3424.

Kim HK, Davaa E, Myung CS, Park JS. 2010. Enhanced siRNA delivery using cationic liposomes with new polyarginine-conjugated PEG-lipid. Int J Pharm 392:141–147.

Kocbek P, Obermajer N, Cegnar M, Kos J, Kristl J. 2007. Targeting cancer cells using PLGA nanoparticles surface modified with monoclonal antibody. J Control Release 120:18–26.

Kovacs T, Karasz A, Szollosi J, Nagy P. 2009. The density of GM1-enriched lipid rafts correlates inversely with the efficiency of transfection mediated by cationic liposomes. Cytometry A 75:650–657.

Liao KW, Chen BM, Liu TB, Tzou SC, Lin YM, Lin KF, Su CI, Roffler SR. 2003. Stable expression of chimeric anti-CD3 receptors on mammalian cells for stimulation of antitumor immunity. Cancer Gene Ther 10:779–790.

Lin WC, Blanchette CD, Ratto TV, Longo ML. 2006. Lipid asymmetry in DLPC/DSPC-supported lipid bilayers: A combined AFM and fluorescence microscopy study. Biophys J 90:228–237.

Lin YL, Lai YJ, Tsai NM, Peng TC, Liu YK, Lee RP, Tsai CJ, Liao KW. 2010. A new microsphere-based immunoassay for measuring the activity of transcription factors. Biol Proced Online 12:18–26.

Mangala LS, Han HD, Lopez-Berestein G, Sood AK. 2009. Liposomal siRNA for ovarian cancer. Methods Mol Biol 555:29–42.

McNeil SE, Vangala A, Bramwell VW, Hanson PJ, Perrie Y. 2010. Lipoplexes formulation and optimisation: In vitro transfection studies reveal no correlation with in vivo vaccination studies. Curr Drug Deliv 7:175–187.

Merritt WM, Lin YG, Spannuth WA, Fletcher MS, Kamat AA, Han LY, Landen CN, Jennings N, De Geest K, Langley RR, Villares G, Sanguino A, Lutgendorf SK, Lopez-Berestein G, Bar-Eli MM, Sood AK. 2008. Effect of interleukin-8 gene silencing with liposome-encapsulated small interfering RNA on ovarian cancer cell growth. J Natl Cancer Inst 100:359–372.

Nobs L, Buchegger F, Gurny R, Allemann E. 2004. Current methods for attaching targeting ligands to liposomes and nanoparticles. J Pharm Sci 93:1980–1992 .

Obata Y, Ciofani G, Raffa V, Cuschieri A, Menciassi A, Dario P, Takeoka S. 2010. Evaluation of cationic liposomes composed of an amino acid-based lipid for neuronal transfection. Nanomedicine 6:70–77.

Ong BC, Leong YK, Chen SB. 2009. Interparticle forces in spherical monodispersed silica dispersions: Effects of branched polyethylenimine and molecular weight. J Colloid Interface Sci 337:24–31.

Pelisek J, Gaedtke L, DeRouchey J, Walker GF, Nikol S, Wagner E. 2006. Optimized lipopolyplex formulations for gene transfer to human colon carcinoma cells under in vitro conditions. J Gene Med 8:186–197.

Rao NM. 2010. Cationic lipid-mediated nucleic acid delivery: Beyond being cationic. Chem Phys Lipids 163:245–252.

Schafer J, Hobel S, Bakowsky U, Aigner A. 2010. Liposome–polyethylenimine complexes for enhanced DNA and siRNA delivery. Biomaterials 31:6892–6900.

Semple SC, Akinc A, Chen J, Sandhu AP, Mui BL, Cho CK, Sah DW, Stebbing D, Crosley EJ, Yaworski E, Hafez IM, Dorkin JR, Qin J, Lam K, Rajeev KG, Wong KF, Jeffs LB, Nechev L, Eisenhardt ML, Jayaraman M, Kazem M, Maier MA, Srinivasulu M, Weinstein MJ, Chen Q, Alvarez R, Barros SA, De S, Klimuk SK, Borland T, Kosovrasti V, Cantley WL, Tam YK, Manoharan M, Ciufolini MA, Tracy MA, de Fougerolles A, MacLachlan I, Cullis PR, Madden TD, Hope MJ. 2010. Rational design of cationic lipids for siRNA delivery. Nat Biotechnol 28:172–176.

Song SX, Liu D, Peng JL, Sun Y, Li ZH, Gu JR, Xu YH. 2008. Peptide ligand-mediated liposome distribution and targeting to EGFR expressing tumor in vivo. Int J Pharm 363:155–161.

Sun YX, Zeng X, Meng QF, Zhang XZ, Cheng SX, Zhuo RX. 2008. The influence of RGD addition on the gene transfer characteristics of disulfide-containing polyethyleneimine/DNA complexes. Biomaterials 29:4356–4365.

Tabatt K, Kneuer C, Sameti M, Olbrich C, Muller RH, Lehr CM, Bakowsky U. 2004. Transfection with different colloidal systems: Comparison of solid lipid nanoparticles and liposomes. J Control Release 97:321–332.

Temming K, Schiffelers RM, Molema G, Kok RJ. 2005. RGD-based strategies for selective delivery of therapeutics and imaging agents to the tumour vasculature. Drug Resist Updat 8:381–402.

Wang H, Zhao P, Su W, Wang S, Liao Z, Niu R, Chang J. 2010. PLGA/polymeric liposome for targeted drug and gene co-delivery. Biomaterials 31(33): 8741–8748.

Weng KC, Noble CO, Papahadjopoulos-Sternberg B, Chen FF, Drummond DC, Kirpotin DB, Wang DH, Hom YK, Hann B, Park JW. 2008. Targeted tumor cell internalization and imaging of multifunctional quantum dot-conjugated immunoliposomes in vitro and in vivo. Nano Lett 8:2851–2857.

Yamada-Ohnishi Y, Azuma H, Urushibara N, Yamaguchi M, Fujihara M, Kobata T, Ikeda H. 2004. Cytotoxic difference of T cells expanded with anti-CD3 monoclonal antibody in the presence and absence of anti-CD 28 monoclonal antibody. Stem Cells Dev 13:315–322.

Yamazaki Y, Nango M, Matsuura M, Hasegawa Y, Hasegawa M, Oku N. 2000. Polycation liposomes, a novel nonviral gene transfer system, constructed from cetylated polyethylenimine. Gene Ther 7:1148–1155.

Zeng J, Wang X, Wang S. 2007. Self-assembled ternary complexes of plasmid DNA, low molecular weight polyethylenimine and targeting peptide for nonviral gene delivery into neurons. Biomaterials 28:1443–1451.

Zhang C, Tang N, Liu X, Liang W, Xu W, Torchilin VP. 2006. siRNA-containing liposomes modified with polyarginine effectively silence the targeted gene. J Control Release 112:229–239.

Zhang L, Gao HG, Chen LF, Wu B, Zheng YR, Liao RX, Jiang Y, He FT. 2008. Tumor targeting of vincristine by mBAFF-modified PEG liposomes in B lymphoma cells. Cancer Lett 269:26–36.

Zhao H, Wang JC, Sun QS, Luo CL, Zhang Q. 2009. RGD-based strategies for improving antitumor activity of paclitaxel-loaded liposomes in nude mice xenografted with human ovarian cancer. J Drug Target 17:10–18.

Zidovska A, Evans HM, Ahmad A, Ewert KK, Safinya CR. 2009. The role of cholesterol and structurally related molecules in enhancing transfection of cationic liposome–DNA complexes. J Phys Chem B 113:5208–5216.